International Journal of Network Dynamics and Intelligence Scilight

Article

String Stable Bidirectional Platooning Control for Heterogeneous Connected Automated Vehicles

Dengfeng Pan*

School of Science, Computing and Engineering Technologies, Swinburne University of Technology, Melbourne, VIC 3122, Australia
* Correspondence: E-mail: dengfengpan@swin.edu.au

Received: 8 August 2024
Accepted: 18 September 2024
Published: 27 December 2024

Abstract: In vehicular platoons, disturbances can be amplified significantly downstream in the platoon if not adequately addressed, potentially leading to traffic jams or collisions. This paper tackles the challenge in maintaining string stability of heterogeneous vehicular platoons under a bidirectional communication topology and a refined constant time headway spacing policy. First, unlike the commonly used constant spacing policy and constant time headway policy, a refined constant time headway policy that combines the benefits of constant spacing and constant time headway policies is presented to enhance platooning safety while maintaining traffic efficiency. Second, a distributed adaptive estimator is designed such that each follower ensures its real-time estimation on the inaccessible leader's full states. The proposed estimators also well accommodate the heterogeneity among vehicles, allowing distinct inertial lag parameters of the vehicle longitudinal dynamics. Third, leveraging a bidirectional communication topology, a distributed scalable platoon controller is developed to guarantee the desired individual stability and string stability requirements of the vehicle platoon without the need of any global information of the communication topology. Formal sufficient conditions are provided on the existence of the desired estimator and controller gains. Finally, numerical simulations are conducted to verify the efficacy of the derived theoretical results. The simulations highlight the string stability and superiority of the proposed spacing policy, demonstrating the effectiveness of the proposed platooning control method.

Keywords: Heterogeneous vehicular platoon; refined constant time headway spacing policy; bidirectional communication; string stability; platooning control

1. Introduction

Almost everyone has experienced traffic jams, but sometimes, the cause of the jam is not immediately apparent–there are no collisions, accidents, or red lights. This type of traffic jams is the so-called phantom jams. They can occur due to a minor yet sudden maneuver of a single driver, such as a slight deceleration to avoid vehicles ahead. As a result, following vehicles have to decelerate or even stop for longer periods to avoid collision, creating a chain-reaction where the initial minor disturbance amplifies down the line of vehicles, forming a phantom jam [1]. Phantom jam was formed because drivers lack timely information from vehicles ahead, so drivers have to take longer time to react to the misbehavior of preceding vehicles. However, advancements in information technology and automobile industry have enabled vehicles to share data with others, allowing for quicker responses to unknown disturbances. Consequently, platooning control of connected automated vehicles has become a hot spot [2–6].

In the field of platooning control, the issue of phantom jams in traffic is addressed by guaranteeing the string stability of platoons. Although string stability has been recognized since 1996 [7], there is still no generally used mathematical definition on it. The literature presents several popular definitions of string stability, including L_2-, L_p- and L_∞-string stability [8–10], prescribed string stability [11], and strict string stability [12, 13]. However, unlike the strict string stability where the string stability is discussed between two adjacent vehicles, studies employing L_2-, L_p- and L_∞-string stability or prescribed string stability often aim to control the propagated disturbance within certain ranges. Such conversions can mitigate the disturbances to some extent, whereas the amplification of disturbances cannot be prevented. Therefore, strict string stability is more preferable as it directly addresses the amplification of disturbances, aligning with the original intention of string stability. Many studies have explored the strict string stability [12, 13], whereas the majority of them focus on the constant time headway (CTH) policy. Analyzing strict string stability in the s-domain is intricately linked to controller design and spacing policy selection. Adapting this analysis to different spacing policies remains challenging. This study aims to bridge this gap by designing platoon controllers that ensure strict string stability under a refined spacing policy.

Two most commonly used spacing policies in the existing vehicle platooning literature are the constant spacing (CS) policy [15, 16] and the CTH policy [17−19], and each has its own advantages and disadvantages. Specifically, the CS policy ensures shorter inter-vehicle gaps than the CTH policy but lacks adaptability to change in vehicle velocities, potentially leading to inefficiencies in tracking predecessor vehicles, especially when leader's acceleration is nonzero or sudden changes in road conditions occur. Conversely, the CTH policy provides smoother adjustments to changes in vehicle velocities but can result in excessively large spacing during high-speed driving. To address these issues, this study explores the refined constant time headway (RCTH) policy proposed in [20], which adjusts the spacing based on the velocity difference between vehicles rather than solely on single vehicle's velocity. This spacing policy enjoys the CS benefits when two vehicles travel at the same velocity and achieves significant traffic efficiency compared to the CTH policy, meanwhile maintaining small gaps than CTH during transient states when two vehicles travel at diverse speeds and preserving significant driving safety than CS. Note that the string stability of vehicular platoons using the RCTH policy was not investigated in [20].

While significant progress have been made in the string stability of vehicular platoons in recent years, much of the research has focused on homogeneous platoons, i.e., the platoon vehicles either are of the same type or possess the same vehicle dynamic parameters in terms of size, weight, length, inertial lag and so on; see, e.g., [8, 9, 12, 13, 21] and references therein. However, real-world vehicles often exhibit heterogeneity due to differences in factors such as brands and loads, which limits the applicability of those results for homogeneous vehicular platoons. Consequently, it is imperative to develop effective control schemes for heterogeneous vehicular platoons to fill this gap. Although some progress has been made to address heterogeneity in vehicular platoons [22]. The platoon control scheme therein typically requires global information about the vehicle-to-vehicle communication topology, which may not always be available in real-world scenarios. Therefore, another motivation of this study is to further develop scalable control schemes that do not require any global information on the communication topology.

Considering the discussion above, this paper focuses on the string stability of heterogeneous vehicular platoons under a bidirectional communication topology and a RCTH spacing policy. The main contributions of this paper are summarized as follows: 1) A RCTH spacing policy which promises to simultaneously enhance the platooning safety and maintain the traffic efficiency. Compared to the widely used CS policy and CTH spacing policy, the RCTH spacing policy provides adaptability to changes in vehicle velocity and allows for smaller spacings than the CTH spacing policy during steady-state driving; 2) A distributed adaptive estimator for each follower vehicle which skillfully handles the heterogeneity in the vehicle platoon and enables real-time estimation of the leader vehicle's unavailable full motion states; and 3) A bidirectional distributed platoon controller that guarantees both provable individual stability and string stability of the concerned platoon. The design of this controller does not require any global information of the communication topology.

The remainder of this paper is organized as follows: Section 2 presents the preliminaries and main problem formulation. Section 3 provides the main results, including the estimator design, controller design, and string stability analysis. Section 4 presents simulations to verify the theoretical results. Finally, conclusions are drawn in Section 5.

2. Preliminaries and Problem Formulation

2.1. Notations

For a matrix in $A \in \mathbb{R}^{m\times n}$, $A^\top$ refers to the transpose of A. $I_N \in \mathbb{R}^{N\times N}$ is the identity matrix. $\mathbf{e}$ denotes the Euler's number. Moreover, $\lambda_{\max}(A)$ and $\lambda_{\min}(A)$ denote the largest and the smallest eigenvalues of the matrix A, respectively.

2.2. Longitudinal vehicle dynamics

Consider a connected vehicle platoon consisting of N followers, indexed by $i = 1, 2, \cdots, N$, and one leader, denoted as vehicle 0. For each follower vehicle i, the following third-order model is commonly adopted to describe the vehicle longitudinal dynamics [23, 24]:

$$\tau_i \dddot{p}_i(t) + \ddot{p}_i(t) = u_i(t),\ i \in \mathcal{V} = \{0,1,2,\cdots,N\}, \tag{1}$$

where $p_i(t) \in \mathbb{R}$ represents the longitudinal position of vehicle i, $\tau_i \in \mathbb{R}^+$ is the unknown heterogeneous inertial lag of the longitudinal vehicle dynamics, and $u_i(t) \in \mathbb{R}$ denotes the desired acceleration control input to be designed for vehicle i. By stacking each vehicle's position and its first- and second-order derivatives into an augmented vector $x_i(t) = [p_i(t), \dot{p}_i(t), \ddot{p}_i(t)]^T$ and denoting $A_i = [0,1,0;0,0,1;0,0,-1/\tau_i]$, $B_i = [0,0,1/\tau_i]^\top$, for any $i \in \cup\mathcal{V}$, then the longitudinal dynamics (1) can be rewritten into a compact state-space form as

$$\dot{x}_i(t) = \quad A_i x_i(t) + B_i u_i(t),\ i \in \mathcal{V}. \tag{2}$$

The leader vehicle also abides by the above longitudinal dynamics but possess an unknown input $u_0(t)$ and a known inertial lag parameter τ_0. The system matrices A_0 and B_0 thus can be similarly derived in terms of τ_0. The leader input $u_0(t)$, on the other hand, is generally unknown to the follower vehicles, which can be deemed as an external disturbance input to the whole platoon. In what follows, we will investigate the string stability of the platoon mainly due to the leader input changes. As shown in Figure 1(a), the platooning tracking error will be greatly amplified (over twice that of the first vehicle) downstream in the platoon, even when there is only a small disturbance in the first vehicle. Conversely, as shown in Figure 1(b), the disturbance in the first vehicle will not be amplified downstream in the platoon if the platoon is string stable, guaranteeing the last vehicle will not deviate from the desired position too much. Due to constraints such as speed limitations and passenger comfort in realistic platooning, the following mild assumption is made on the platoon leader input.

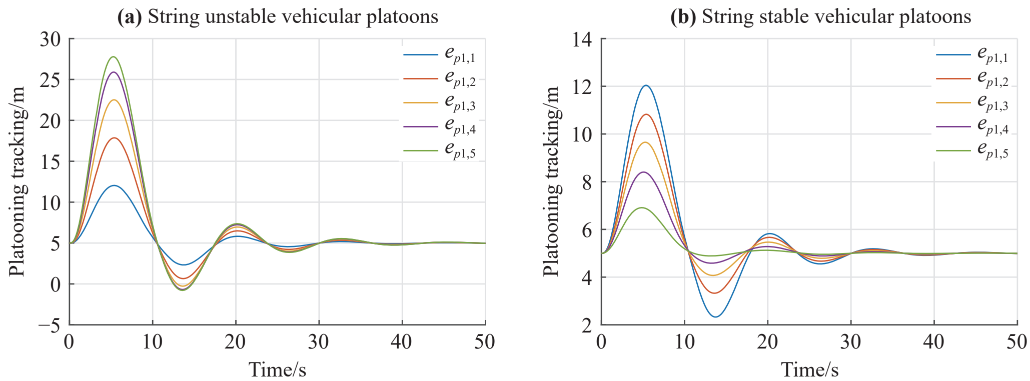

Figure 1. Platooning tracking errors of string unstable and string stable vehicular platoons with the safety distance being 5 m, where $e_{p1,i}(t) = p_0(t) - p_i(t)$. (a) String unstable vehicular platoons; (b) string stable vehicular platoons.

Assumption 1. *The input of the leader is unknown but bounded, i.e.,* $|u_0(t)| < \bar{u}_0$ *with* $\bar{u}_0$ *being an unknown positive scalar.*

2.3. A refined constant time headway spacing policy

Figure 2 provides an illustration of an ideal vehicular platoon consisting of 4 followers and one leader. The safety distance between the leader and the ith follower is denoted as $\bar{d}_i^*$, the spacing between the ith and jth followers is denoted as $\bar{d}_{i,j}^*$, and the velocity of the ith follower is denoted as $\dot{p}_i(t)$. Motivated by [20], we adopt the following RCTH spacing policy in this study, which can be described as

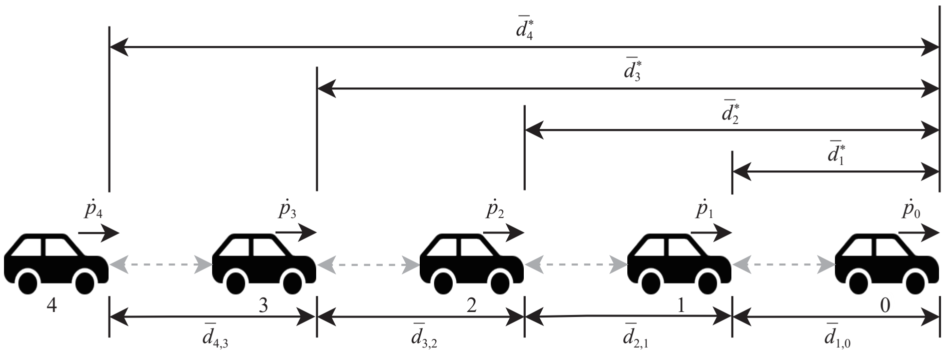

Figure 2. Illustration of an ideal vehicular platoon consisting of four followers and one leader.

$$\bar{d}_{i,j}(t) = \quad \bar{d}_i^* - \bar{d}_j^* + h(\dot{p}_i(t) - \dot{p}_j(t)),\ i,j \in \mathcal{V}, \tag{3}$$

where $\bar{d}_i^* > 0$ (or $\bar{d}_j^* > 0$ respectively) is the safety distance between the ith (or jth) follower and the leader, and $h > 0$ is the prescribed headway time (in seconds). Additionally, for ease of analysis, define $d_{i,j}^* = [\bar{d}_i^* - \bar{d}_j^*, 0, 0]^\top$ and $d_{i,j}(t) = [\bar{d}_{i,j}(t), 0, 0]^\top$.

Remark 1. *The platooning control literature extensively examines two spacing strategies: constant spacing (CS) policies and constant time headway (CTH) policies. CS policies maintain a fixed distance between vehicles, while CTH policies determine spacing based on a specified time headway and real-time vehicle velocity. Generally, CS policies result in tighter spacing, whereas CTH policies prioritize safety, especially at higher velocities. However, at faster velocities, CTH policies can lead to greater distances between vehicles, potentially reducing traffic efficiency. To address this issue, it is crucial to account for velocities of neighboring vehicles. Equation* (3) *shows that, in RCTH, vehicle spacing is influenced by the velocity difference between vehicles i and j, not just the velocity of vehicle i. This can significantly reduce spacing upon platoon formation and improve collision avoidance capabilities. For example, if vehicle i is moving faster than vehicle j, the spacing between them will increase, enhancing traffic safety; and if vehicle i is moving slower than vehicle j, the spacing between them will decrease, forcing vehicle i catch up vehicle j. When vehicle i and j run in the same velocity, the spacing between them will be kept constant.*

Remark 2. *A small simulation is conducted to compare different spacing policies with the the predecessor's velocity set at 10 m/s, illustrating the superiority of the proposed RCTH policy. The results are shown in* Fig. 3. *As depicted, the spacings between vehicles remain constant under the CS policy, while the spacings are adjusted according to vehicle velocity under the CTH and RCTH policies. The spacings under the CTH policy, however, are consistently larger than those under the RCTH policy, demonstrating that the RCTH policy maintains tighter spacings compared to the CTH policy. Additionally, when the velocity of the ego vehicle matches that of the predecessor, the spacings under the RCTH policy are the same as those under the CS policy. This highlights the flexibility and adaptability of the RCTH policy in maintaining tight spacings between vehicles while ensuring traffic safety and efficiency.*

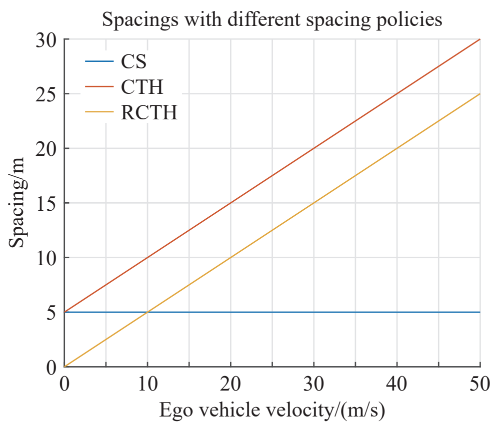

Figure 3. Spacing of vehicular platoons applying CS, CTH and RCTH policies with a headway time $h = 0.5$ s when the predecessor is traveling at 10 m/s.

2.4. Distributed adaptive estimators

The heterogenous inertial lag τ_i in the longitudinal vehicle dynamics (1) on each follower vehicle i is often unknown to its neighbors. This makes the subsequent platoon controller design and stability analysis quite challenging. Moreover, due to the unknown leader input $u_0(t)$, the leader's full state $x_0(t)$ is inaccessible to all follower vehicles, which calls for a suitable distributed observer [25] for each follower to estimate the full leader state. In the sequel, by leveraging the known information of the leader vehicle's inertial lag parameter, or equivalently known A_0, B_0, and bidirectional vehicle-to-vehicle communication, we are interested in constructing and designing the following distributed adaptive estimator:

$$\begin{cases} \dot{\theta}_i(t) = A_0\theta_i(t) + B_0K_h\iota_{i,i-1}(t)w_{i,i-1}(t) + B_0K_h\iota_{i,i+1}(t)w_{i,i+1}(t) \\ \dot{\iota}_{ij}(t) = -\kappa_{ij}\left(\upsilon_{ij}\iota_{ij}(t) - w_{ij}^\top(t)\Gamma w_{ij}(t)\right), j = \{i-1, i+1\} \end{cases} \tag{4}$$

where $\theta_i(t)$ is the estimation of the leader's state $x_0(t)$ by the ith follower, $\iota_{ij}(t)$ is the adaptive coupling gain with regard to the edge $(i,j) \in \mathcal{E}$, $w_{ij}(t) = \theta_i(t) - \theta_j(t)$, $\kappa_{ij} = \kappa_{ji}$ and $\upsilon_{ij} = \upsilon_{ji}$ are prescribed positive constants, K_h and $\Gamma \geqslant 0$ are gain matrices to be designed and $c > 0$ is the coupling gain to be specified later. Besides, for the purpose of unifying notations to simplify the proof, we define $\theta_0(t) = x_0(t)$. Furthermore, initializing the adaptive coupling gain as $\iota_{ij}(0) = \iota_{ji}(0) > 0$, one has $\iota_{ij}(t) = \iota_{ji}(t) > 0$ because the parameter $\kappa_{ij}a_{ij}\upsilon_{ij} \geqslant 0$.

Define the estimation error as $e_{h,i}(t) = \theta_i(t) - x_0(t)$ for any $i \in \mathcal{V}$. Based on (2) and (4), the error dynamics can be derived as follows

$$\dot{e}_{h,i}(t) = \quad A_0 e_{h,i}(t) + B_0 K_h(\iota_{i,i-1}(t) w_{i,i-1}(t) + \iota_{i,i+1}(t) w_{i,i+1}(t)) - B_0 u_0(t). \tag{5}$$

2.5. Bidirectional scalable platoon controllers

Denote $E_2 = [0,h,0;0,0,0;0,0,0]$ and $E_3 = [0,0,h;\ 0,0,0;0,0,0]$. For any $i \in \mathcal{V}$, we define the longitudinal platooning tracking error and its first and second derivatives as $e_{p1,i}(t) = p_i(t) - p_0(t) + \bar{d}_i^*$ and $e_{p3,i}(t) = \dot{e}_{p2,i}(t) = \ddot{e}_{p1,i}(t)$. Based on the estimations from estimator (4), the following bidirectional scalable platoon controller is deigned for each follower i:

$$\begin{aligned} u_{a,i}(t) = &-\tau_i k_1(p_i(t) - \theta_{i1}(t) + \bar{d}_i^* + (h+k_4)(\dot{p}_i(t) - \dot{\theta}_{i1}(t)) + k_5(\ddot{p}_i(t) - \ddot{\theta}_{i1}(t))) \\ &- \tau_i k_2(e_{p1,i}(t) - e_{p1,i-1}(t) + (h+k_4)(e_{p2,i}(t) - e_{p2,i-1}(t)) + k_5(e_{p3,i}(t) - e_{p3,i-1}(t)) \\ &- \tau_i k_3(e_{p1,i}(t) - e_{p1,i+1}(t) + (h+k_4)(e_{p2,i}(t) - e_{p2,i+1}(t)) + k_5(e_{p3_i}(t) - e_{p3,i+1}(t)) - \frac{\tau_i - \tau_0}{\tau_0}\ddot{p}_i(t) \end{aligned} \tag{6}$$

where $k_1 > 0$, $k_2 > 0$, $k_3 > 0$, $k_4 > 0$, $k_5 > 0$ are gains to be determined. Here, by 'bidirectional' we mean that each follower vehicle i employs information from not only itself but also from both its direct predecessor $i-1$ and successor $i+1$, namely, bidirectional vehicle-to-vehicle communication [26]; by 'scalable' we mean that the design of the above platoon controller gain parameters is independent of any global communication topology information, which will be shown in Theorem 2.

2.6. The problem to be addressed

Stacking the platooning tracking errors into an augmented vector $e_{p,i} = [e_{p1,i}(t), e_{p2,i}(t), e_{p3,i}(t)]^\top$ and recalling the spacing policy (3) and controller (6), the longitudinal platooning tracking error dynamics can be written as

$$e_{p,i}(t) = \quad E_4 e_{h,i} + (A_0 - KE_4)e_{p,i}(t) + k_2 E e_{p,i-1}(t) + k_3 E_4 e_{p,i+1}(t) \tag{7}$$

with $K = k_1 + k_2 + k_3$, $E_4 = \begin{bmatrix} 0 & 0 & 0 \\ 0 & 0 & 0 \\ 1 & h+k_4 & k_5 \end{bmatrix}$, which can be further rewritten as

$$\dot{\bar{e}}_p(t) = \bar{A}\bar{e}_p(t) + (E_4 \otimes I)\bar{e}_h(t), \tag{8}$$

where

$$\begin{aligned} \bar{e}_p(t) =& [e_{p1,1}(t), e_{p1,2}(t), \cdots, e_{p1,N}(t), e_{p2,1}(t), e_{p2,2}(t), \cdots, \\ & e_{p2,N}(t), e_{p3,1}(t), e_{p3,2}(t), \cdots, e_{p3,N}(t)]^\top, \\ \bar{e}_h(t) =& [e_{h1,1}(t), e_{h1,2}(t), \cdots, e_{h1,N}(t), e_{h2,1}(t), e_{h2,2}(t), \cdots, \\ & e_{h2,N}(t), e_{h3,1}(t), e_{h3,2}(t), \cdots, e_{h3,N}(t)], \\ \bar{A} =& A_0 \otimes I_N - E_4 \otimes (k_1 I_N + \mathcal{K}) \\ \mathcal{K} =& \begin{bmatrix} k_2+k_3 & -k_3 & 0 & 0 & \cdots & 0 \\ -k_2 & k_2+k_3 & -k_3 & 0 & \cdots & 0 \\ 0 & -k_2 & k_2+k_3 & -k_3 & \cdots & 0 \\ \vdots & \vdots & \vdots & \vdots & \vdots & 0 \\ 0 & 0 & 0 & 0 & \cdots & k_2 \end{bmatrix} \in \mathbb{R}^{N\times N} \end{aligned}$$

The definition of string stability is given as follows.

Definition 1. [27] *For vehicular platoons consisting of N follower vehicles, indexed by $i = 1,2,...,N$, and one leader vehicle, denoted as $i = 0$, the platoon is considered string stable if the transfer function of tracking errors between vehicles i and its predecessor $i-1$, denoted as $G_i(s) = e_{p,i}(s)/e_{p,i-1}(s)$, satisfies the following condition:*

$$\|G_i(s)\|_{H_\infty}^{[0,\infty)} < 1, \forall i = 1,2,\cdots,N, \tag{9}$$

where $s = \jmath\omega$ with $\jmath = \sqrt{-1}$ being the imaginary unit and ω being the frequency.

We aim to fulfill the following objectives in this study:

● *(Distributed adaptive estimation)*: Design a distributed adaptive estimator in the form of (4) for each vehicle i to estimate the leader's state such that the estimation error (5) is ultimately bounded, i.e., $\lim_{t\to\infty}\|e_{h,i}(t)\| \le \chi_1$ with χ_1 being a positive scalar;

• *(Platoon individual stability and strict string stability)*: Design a bidirectional scalable platoon controller in the form of (6) for each vehicle i such that, under the employed RCTH policy (3), the longitudinal platooning tracking error is not only ultimately bounded, specifically, $\lim_{t\to\infty}\|e_{p,i}(t)\|\leqslant\chi_2$ with χ_2 being a positive scalar, but also not amplified downstream in the platoon, i.e., $\|e_{p,i}(t)\|_\infty/\|e_{p,i-1}(t)\|_\infty<1$.

Lemma 1. [28] *For continuous function $f(t)$ satisfying $\lim_{t\to\infty}f(t)=0$ and $|f(t)|<\infty$, one has*

$$\lim_{t\to\infty}\int_0^t \mathbf{e}^{-a(t-\tau)}|f(\tau)|d\tau=0, \tag{10}$$

where a is a positive scalar.

Corollary 1. *For continuous function $f(t)$ satisfying $\lim_{t\to\infty}f(t)=c$ with c being a constant and $|f(t)|<\infty$, one has*

$$\lim_{t\to\infty}\int_0^t \mathbf{e}^{-a(t-\tau)}|f(\tau)|d\tau\leqslant\tfrac{|c|}{a}, \tag{11}$$

where a is a positive scalar.

Proof of Corollary 1. Divide $f(x)$ into two parts as $f(x)=g(x)+c$ with $\lim_{t\to\infty}g(x)=0$. Then,

$$\begin{aligned}\lim_{t\to\infty}\int_0^t \mathbf{e}^{-a(t-\tau)}|f(\tau)|d\tau &=\lim_{t\to\infty}\int_0^t \mathbf{e}^{-a(t-\tau)}|g(\tau)+c|d\tau\\ &\leqslant\lim_{t\to\infty}\int_0^t \mathbf{e}^{-a(t-\tau)}|g(\tau)|d\tau+\lim_{t\to\infty}\int_0^t \mathbf{e}^{-a(t-\tau)}|c|d\tau\end{aligned}$$

Recalling Lemma 1 and noticing that $\lim_{t\to\infty}\int_0^t \mathbf{e}^{-a(t-\tau)}|c|d\tau=\dfrac{|c|}{a}$, one has

$$\lim_{t\to\infty}\int_0^t \mathbf{e}^{-a(t-\tau)}|f(\tau)|d\tau\leqslant\frac{|c|}{a}.$$

The proof is complete.

3. Main results

In this section, the desired distributed adaptive estimator is first designed to guarantee that the local estimation error is ultimately bounded. After that, sufficient conditions are derived to determine the gains of the proposed bidirectional scalable platoon controllers, where an analysis of both individual and string stability for the controlled platoon is also provided.

3.1. Distributed adaptive estimator design

The design criterion of the estimator (4) is stated in the following theorem.

Theorem 1. *Under the estimator* (4), *the local estimation error* (5) *is uniformly ultimately bounded if there exist positive definite matrices P and Q such that*

$$PA_0+A_0^\top P-PB_0B_0^\top P+Q=0 \tag{12}$$

hold. Additionally, the estimator gain matrix K_h can be designed as $K_h=-B_0^\top P$.

Proof of Theorem 1. Select the Lyapunov function candidate as

$$V(t)=\sum_{i=1}^N e_{h,i}^\top(t)Pe_{h,i}(t)+\sum_{i=1}^N\sum_{j=i-1}^{i+1}\frac{\bar{\iota}_{ij}^2(t)}{2\kappa_{ij}},$$

where $\bar{\iota}_{ij}(t)=\iota_{ij}(t)-\epsilon_1$ with $\epsilon_1>0$ being a scalar to be determined later.

The time derivative of $V(t)$ along (4) and (5) is

$$\begin{aligned}\dot V(t)=&2\sum_{i=1}^N e_{h,i}^\top(t)PA_0e_{h,i}(t)-\sum_{i=1}^N e_{h,i}^\top(t)PB_0u_0(t)\\ &-\sum_{i=1}^N\sum_{j=i-1}^{i+1}\frac{\bar{\iota}_{ij}(t)}{2}\upsilon_{ij}\iota_{ij}(t)-\epsilon_1\sum_{i=1}^N\sum_{j=i-1}^{i+1}\frac12 w_{ij}^\top(t)\Gamma w_{ij}(t)\end{aligned}$$

Noting the fact that

$$-\frac12\bar{\iota}_{ij}\iota_{ij}\leqslant-\frac12\iota_{ij}^2+\frac12\epsilon_1^2,$$

selecting $\epsilon_1 = 2/\lambda_{\min}(\mathcal{L})$, where

$$\mathcal{L} = \begin{bmatrix} 2 & -1 & 0 & 0 & \cdots & 0 \\ -1 & 2 & -1 & 0 & \cdots & 0 \\ 0 & -1 & 2 & -1 & \cdots & 0 \\ \vdots & \vdots & \vdots & \vdots & \vdots & 0 \\ 0 & 0 & 0 & 0 & \cdots & 1 \end{bmatrix} \in \mathbb{R}^{N\times N},$$

and in light of Young's inequality, one has

$$\begin{aligned}\dot{V}(t) =& e_h^\top(t)(I_N \otimes (PA_0 + A_0^\top P - PB_0B_0^\top P)e_h(t) \\ & -\sum_{i=1}^{N}\sum_{j=i-1}^{i+1} a_{ij}\upsilon_{ij}\iota_{ij}^2(t) + \sum_{i=1}^{N}\sum_{j=i-1}^{i+1} a_{ij}\upsilon_{ij}\epsilon_1^2 + \sum_{i=1}^{N} u_0^\top(t)u_0(t),\end{aligned}$$

where $e_h(t) = [e_{h,1}(t), e_{h,2}(t), \cdots, e_{h,N}(t)]^\top$, and $a_{ij} = 1$ if the element in the ith row and jth column of $\mathcal{L}$ equals -1, otherwise, $a_{ij} = 0$.

Then if there exists a positive definite matrix Q such that

$$PA_0 + A_0^\top P - PB_0B_0^\top P + Q = 0$$

holds, one has

$$\dot{V}_1(t) \leqslant -\epsilon_2 V(t) + \sum_{i=1}^{N}\sum_{j=1}^{N} a_{ij}\upsilon_{ij}\epsilon_1^2 + \sum_{i=1}^{N} \bar{u}_0^2$$

with $\epsilon_2 = \max\{\lambda_{\max}(P)/\lambda_{\min}(Q), 1/2(a_{ij}\upsilon_{ij}\kappa_{ij})\}$, which, together with $V_1(t) \geqslant 0$, implies that

$$\lim_{t\to\infty} \|e_h(t)\|^2 \leqslant \chi_1,$$

where $\chi_1 = (\sum_{i=1}^{N}\sum_{j=1}^{N} a_{ij}\upsilon_{ij}\epsilon_1^2 + \sum_{i=1}^{N}\bar{u}_0^2)/(\epsilon_2\|P\|)$. The proof is therefore completed.

3.2. Bidirectional scalable platoon controller design

We are now in a position to present a sufficient condition for the controller design that guarantees both individual and string stability of the controlled platoon.

Theorem 2. *Consider the estimator* (4)*, with parameters determined according to the condition developed in Theorem 3.1. The longitudinal tracking error is ultimately bounded and the string stability of platoons* (2) *can be guaranteed under the RCTH spacing policy* (3) *and the estimation-based controller* (6)*, provided that the control gains satisfy the following inequalities:*

$$k_5 > \frac{1}{\tau_0 k_1} \tag{13a}$$

$$k_5 > \frac{\tau_0 k_1 + h + k_4}{\tau_0 k_1 (h + k_4)} \tag{13b}$$

$$k_1 + k_3 > (2\sqrt{2} - 1)k_2, \tag{13c}$$

$$k_1 + k_2 > (2\sqrt{2} - 1)k_3, \tag{13d}$$

$$k_5 > (h + k_4)\tau_0. \tag{13e}$$

Proof of Theorem 2. The proof of Theorem 3.2 is divided into two parts: individual stability and string stability.

<u>*Individual stability*</u>

According to (8), it is straightforward to derive that:

$$\|\bar{e}_p(t)\| \leqslant \mathbf{e}^{\lambda_{\max}(\bar{A})t}\|\bar{e}_p(0)\| + \int_{t_0}^{t} \mathbf{e}^{\lambda_{\max}(\bar{A})(t-\tau)}\|(E_4 \otimes I)\|\|e_{h,i}(\tau)\| d\tau.$$

Recalling that $\lim_{t\to\infty} e_{h,i}(t) \leqslant \chi_1$, and according to Corollary 1, if all the eigenvalues of $\bar{A}$ have negative real parts, then $\lim_{t\to\infty} \bar{e}_p(t) \leqslant \chi_2$, where $\chi_2 = \dfrac{\chi_1}{|\lambda_{\max}(\bar{A})|}$.

In what follows, our aim is to establish a sufficient condition such that all the eigenvalues of $\bar{A}$ have negative real parts. Notably, the characteristic polynomial of $\bar{A}$ can be obtained as:

$$\det(sI-\bar{A}) = \prod_{i=1}^{N}\left(s^3 + (-\frac{1}{\tau_0} + k_1k_5 + k_5\lambda_i(\mathcal{K})\right)s^2 \\ + ((h+k_4)(k_1+\lambda_i(\mathcal{K})))s + k_1 + \lambda_i(\mathcal{K})).$$

Then, the Routh table can be constructed as follows with $\bar{K} = k_1 + \lambda_i(\mathcal{K})$,

According to the classic yet powerful Routh-Hurwitz criteria, if all elements in the first column of the Routh table are positive, then the real parts of the eigenvalues of $\bar{A}$ are all negative. In other words, if the following inequalities are satisfied:

$$k_1 > -\lambda_i(\mathcal{K}) \tag{14}$$

$$k_5 > \frac{1}{\tau_0(k_1+\lambda_i(\mathcal{K}))} \tag{15}$$

$$k_5 > \frac{\tau_0(k_1+\lambda_i(\mathcal{K})) + h + k_4}{\tau_0(k_1+\lambda_i(\mathcal{K}))(h+k_4)} \tag{16}$$

then all the eigenvalues of $\bar{A}$ will have negative real parts. Additionally, according to the Gerschgorin circle theorem, eigenvalues of $\mathcal{K}$ are positive, then one can conclude that (14) always holds. Moreover, since $\lambda_i(\mathcal{K}) > 0$, (15) and (16) can be simplified to (13a) and (13b), respectively.

String stability

Now, we are in a position to prove the string stability of the platoon. For ease of illustration, we set the estimation error $e_{h,i}(t) = 0$. The Laplace transform of (7) is

$$(s^3 + \frac{s^2}{\tau_0} + KH(s))E_{p1,i}(s) = k_2H(s)E_{p1,i-1}(s) + k_3H(s)E_{p1,i+1}(s) \tag{17}$$

with $K = k_1 + k_2 + k_3$ and $H(s) = 1 + (h+k_4)s + k_5s^2$.

By dividing both sides of (17) with $E_{p1,i-1}(s)$, and observing that

$$\frac{E_{p1,i+1}(s)}{E_{p1,i-1}(s)} = \frac{E_{p1,i+1}(s)}{E_{p1,i}(s)}\frac{E_{p1,i}(s)}{E_{p1,i-1}(s)}$$

one obtains:

$$G_i(s) = \frac{E_{p1,i}(s)}{E_{p1,i-1}(s)} = \frac{\frac{k_2H(s)}{s^3+\frac{s^2}{\tau_0}+KH(s)}}{1-\frac{k_3H(s)}{s^3+\frac{s^2}{\tau_0}+KH(s)}\frac{E_{p1,i+1}(s)}{E_{p1,i}(s)}}.$$

Similarly, for the head and tail of the followers, one has

$$G_N(s) = \frac{E_{p1,i}(s)}{E_{p1,i-1}(s)} = \frac{k_2H(s)}{s^3+\frac{s^2}{\tau_0}+KH(s)}$$
$$G_1(s) = \frac{E_{p1,i}(s)}{E_{p1,i-1}(s)} = \frac{k_3H(s)}{s^3+\frac{s^2}{\tau_0}+KH(s)}$$

Note that the conditions for the head and tail of the followers are included in the conditions for the followers in the middle. Therefore, only the sufficient conditions guaranteeing that $||G_1(s)||_{H_\infty}^{[0,\infty)} < 1$ and $||G_N(s)||_{H_\infty}^{[0,\infty)} < 1$ are required. One possible sufficient condition for ensuring that $||G_i(s)||_{H_\infty}^{[0,\infty)} < 1$ is as follows:

$$\left\|\frac{k_2H(s)}{s^3+\frac{s^2}{\tau_0}+KH(s)}\right\|_{H_\infty}^{[0,\infty)} < \frac{1}{2}, \tag{18a}$$

$$\left\|\frac{k_3H(s)}{s^3+\frac{s^2}{\tau_0}+KH(s)}\right\|_{H_\infty}^{[0,\infty)} < \frac{1}{2}. \tag{18b}$$

For (18a), recalling that $s = \jmath w$ with $\jmath = \sqrt{-1}$, one has

$$w^6+\left(\left(\frac{1}{\tau_0}+Kk_5\right)^2-2K(h+k_4)-4k_2^2k_5^2\right)w^4+\left(K\left(\frac{1}{\tau_0}+Kk_5\right)\right.$$
$$\left.+K^2(h+k_4)^2+4k_2^2(h+k_4)^2-8k_2^2k_5\right)w^2+K^2-4k_2^2>0$$

Then, by simple mathematical transformation, it is easy to verify that if (13c)-(13e) hold, then (18a) and (18b) hold. The proof is therefore completed. ■

4. Simulation

This section provides simulation results of one leader and five followers under a bidirectional vehicle-to-vehicle communication topology to verify the effectiveness of the proposed control scheme. For simulation purposes, the inertial lag of each vehicle in the platoon is chosen as $\tau_0=0.46$, $\tau_1=0.52$, $\tau_2=0.58$, $\tau_3=0.64$, $\tau_4=0.70$, $\tau_5=0.76$, and the initial states of each vehicle are set as $x_0(0)=[25,10,0]^\top$, $x_1(0)=[20,10,0]^\top$, $x_2(0)=[15,10,0]^\top$, $x_3(0)=[10,10,0]^\top$, $x_4(0)=[5,10,0]^\top$, $x_5(0)=[0,10,0]^\top$. Besides, the safety distance $\bar{d}_i^*$ is designated to be 5m, and the headway time h is set to be 0.5s. Moreover, the input of the leader is assumed to be in $u_0(t)=4\text{m/s}^2$ during $[0,10]$s, and $u_0(t)=-4$ m/s^2 during $[40,50]$s. The changes of leader acceleration inputs will be regarded as a type of external disturbance to the entire platoon, for which we will examine its string stability performance. For the estimator, the parameters are chosen as $\kappa_{ij}=0.004$ and $\upsilon=0.07$, respectively.

4.1. Effectiveness of the proposed bidirectional platooning control scheme

We first conduct simulation experiments to verify the effectiveness of the proposed control scheme. The results are provided in Figures 4-5. It can be easily observed from Figure 4 that the proposed control scheme can effectively stabilize the platoon and guarantee string stability. Besides, it should be highlighted that the strict string stability against leader acceleration changes can be observed from Figure 4(b), where the position tracking error with regard to each vehicle's direct predecessor is not amplified downstream in the platoon, even when the leader accelerates and decelerates. The time responses of the estimator are illustrated in Figure 5. It is evident that the estimator identifies the leader's real-time motion state well. Additionally, the adaptive coupling gains $\iota_{ij}(t)$ are depicted in Figure 5(d), showcasing their convergence to finite values.

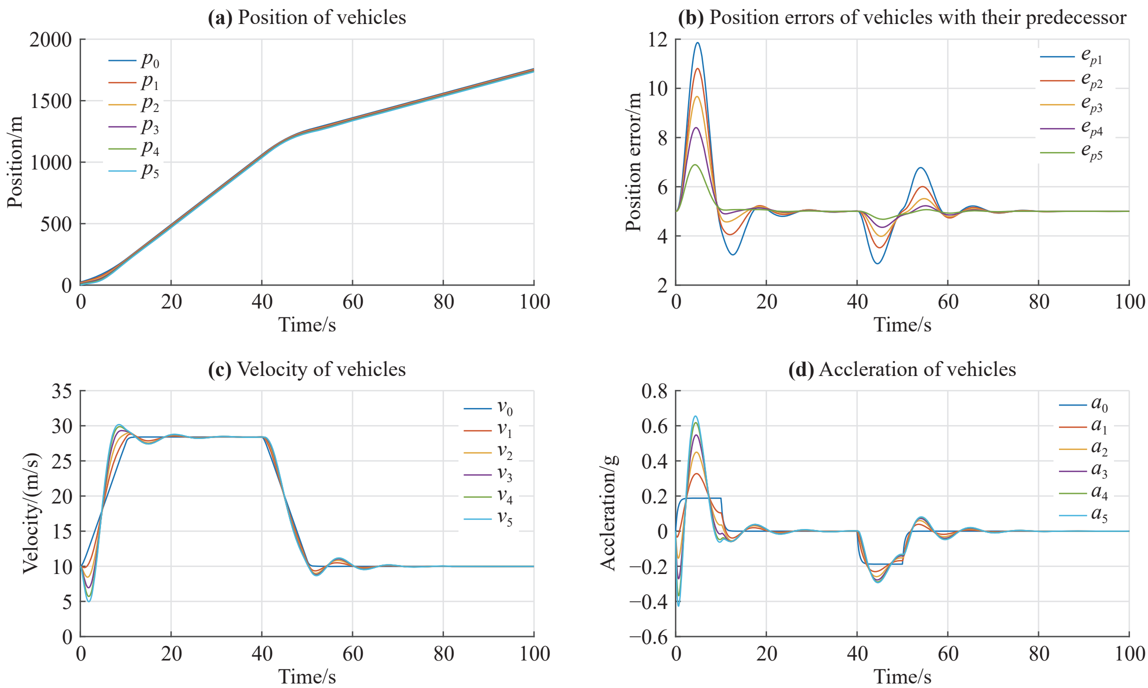

Figure 4. States of vehicles applying controller (6) with the headway time $h=0.5$ s and estimator (4). (a) Vehicles' position; (b) Vehicle's position tracking error with regard to their direct predecessor; (c) Vehicle's velocity; (d) Vehicle's acceleration.

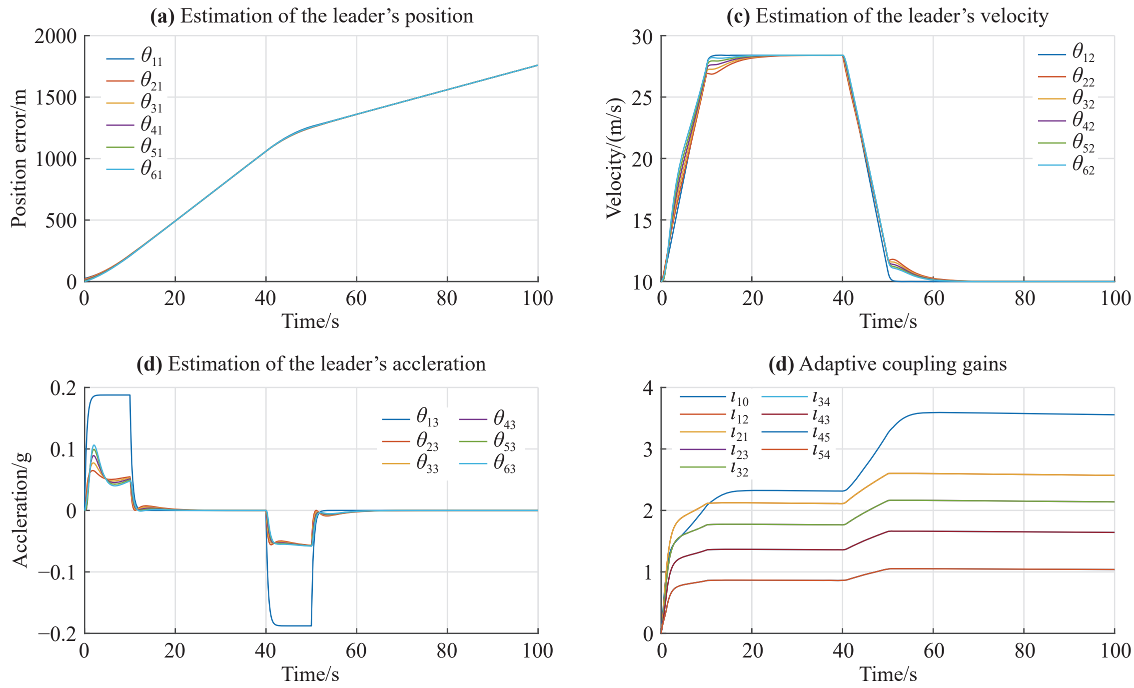

Figure 5. Time responses of the estimator (4). (a) Estimation of the leader's position θ_{i1}; (b) Estimation of the leader's velocity θ_{i2}; (c) Estimation of the leader's acceleration θ_{i3}; (d) Adaptive coupling gains $\iota_{ij}(t)$.

4.2. Comparison between different spacing policies

To showcase the superiority of the proposed RCTH policy, we compare it with two widely used spacing policies, including the CTH policy and the CS policy. The simulation for the CS policy is conducted by setting the headway time in our study to be 0s. However, the proposed RCTH does not lead to CTH straightforwardly due to the adopted relative speed error, we employ the CTH-based platoon controller from [29] as a benchmark. The comparative simulation results are provided in Figure 6-7. It can be observed that with our scheme, string stability is maintained even when the headway time is set to zero. However, as shown in Figure 6, the fluctuation of spacings between vehicles persists much longer with the CS policy than with the proposed RCTH policy. Additionally, the

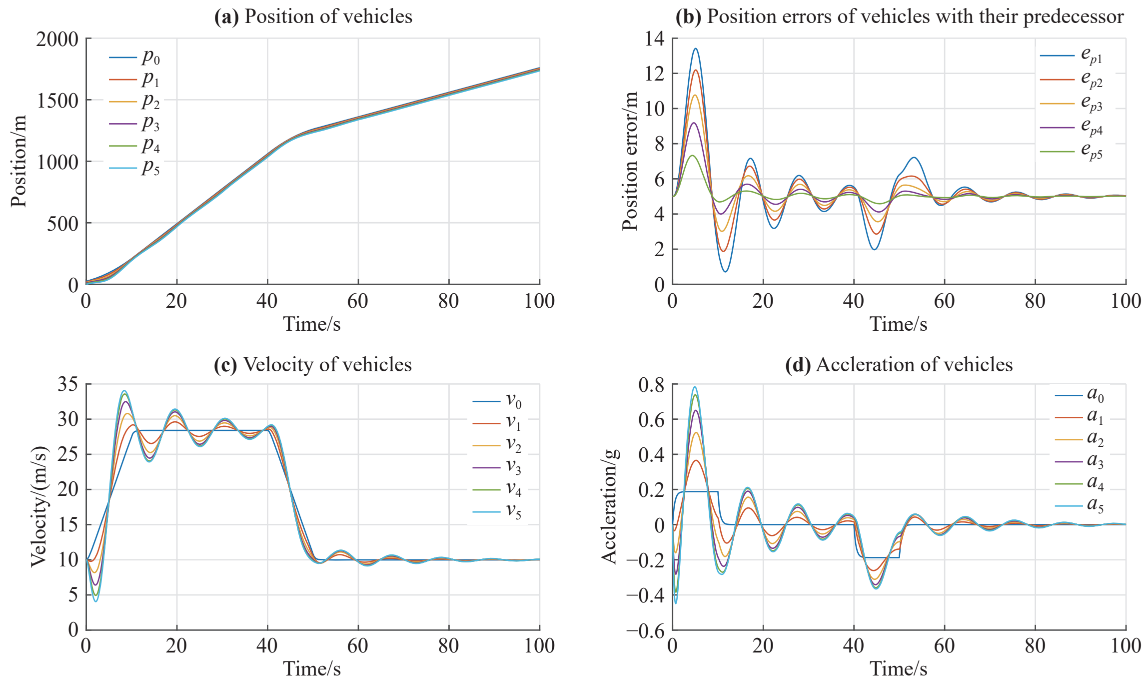

Figure 6. States of vehicles applying controller (6) with the headway time $h = 0$ s and estimator (4). (a) Vehicles' position; (b) Vehicle's position tracking error with regard to their direct predecessor; (c) Vehicle's velocity; (d) Vehicle's acceleration.

maximum spacings between vehicles become larger with the CS policy than with the proposed RCTH policy. For the CTH policy, although the trend of the spacings between vehicles is relatively flat, the spacings are much larger than those with the CS policy and the proposed RCTH policy. As shown in Figure 7(b), the spacings between vehicles surge to 19.2 m when the vehicle velocity is 28.4 m/s, which is much higher than the maximum spacings 13.4172 m of CS policy and the 11.862 m of RCTH policy. Moreover, even when vehicles decelerate to 10 m/s, the spacings between vehicles remain at 10 m, which is twice the safety distance. Summarizing these observations, the proposed RCTH policy is more effective in maintaining the desirable spacings, which matches our previous discussion.

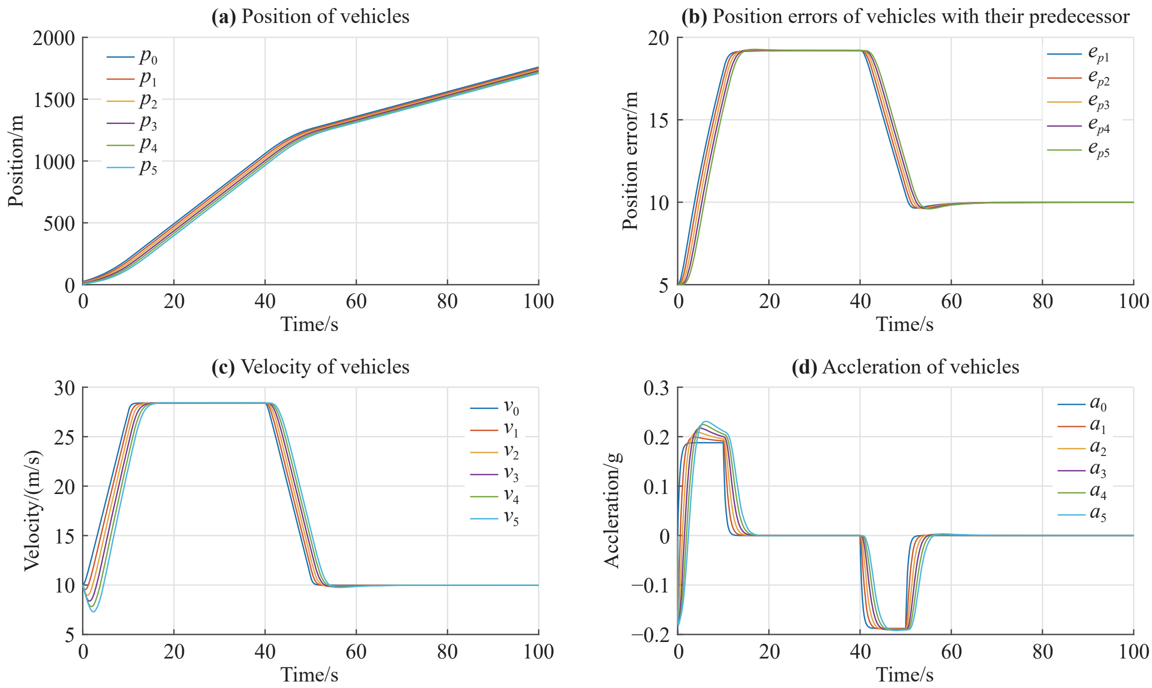

Figure 7. States of vehicles applying controller in [29] with headway time $h = 0.5$ s and estimator (4). (a) Vehicles' position; (b) Vehicle's position tracking error with regard to their direct predecessor; (c) Vehicle's velocity; (d) Vehicle's acceleration.

5. Conclusion

This paper focuses on the individual and string stability of heterogeneous vehicular platoons under the RCTH policy. An estimator is first designed to estimate the states of the leader to enable all following vehicles to have their own estimation of the leader's states. After that, a controller is designed with several conditions to guarantee the individual and string stability of the vehicular platoon under the RCTH policy based on the estimated states. Different from previous work, where the CS policy and CTH policy are utilized, the RCTH policy makes a trade-off between the advantages and drawbacks of these two spacing policies by introducing the velocity differences between vehicles. Finally, a simulation result is provided to verify the feasibility of the proposed control scheme. In our future work, we will focus on 2-D platooning control, where the lateral behavior of vehicular platoons is also a concern.

Data Availability Statement: Not applicable.

Conflicts of Interest: The authors declare no conflicts of interest.

References

1. Won, M.; Park, T.; Son, S. H. Toward mitigating phantom jam using vehicle-to-vehicle communication. IEEE Trans. Intell. Transp. Syst., **2017**, *18*: 1313−1324. doi: 10.1109/TITS.2016.2605925
2. Wang, Y.M.; Liu, W.B.; Wang, C.; *et al*. A novel multi-objective optimization approach with flexible operation planning strategy for truck scheduling. Int. J. Network Dyn. Intell., **2023**, *2*: 100002. doi: 10.53941/ijndi.2023.100002
3. Wang, Z.R.; Bian, Y.G.; Shladover, S.E.; *et al*. A survey on cooperative longitudinal motion control of multiple connected and automated vehicles. IEEE Intell. Transp. Syst. Mag., **2020**, *12*: 4−24. doi: 10.1109/MITS.2019.2953562
4. Guanetti, J.; Kim, Y.; Borrelli, F. Control of connected and automated vehicles: State of the art and future challenges. Annu. Rev. Control, **2018**, *45*: 18−40. doi: 10.1016/j.arcontrol.2018.04.011

5. Jia, D.Y.; Lu, K.J.; Wang, J.P.; *et al*. A survey on platoon-based vehicular cyber-physical systems. IEEE Commun. Surv. Tutorials, **2016**, *18*: 263−284. doi: 10.1109/COMST.2015.2410831
6. Ge, X.H.; Han, Q.L.; Wu, Q.; *et al*. Resilient and safe platooning control of connected automated vehicles against intermittent denial-of-service attacks. IEEE/CAA J. Autom. Sin., **2023**, *10*: 1234−1251. doi: 10.1109/JAS.2022.105845
7. Swaroop, D.; Hedrick, J. K. String stability of interconnected systems. IEEE Trans. Autom. Control, **1996**, *41*: 349−357. doi: 10.1109/9.486636
8. Zhao, Y.; Liu, Z.C.; Wong, W. S. Resilient platoon control of vehicular cyber physical systems under dos attacks and multiple disturbances. IEEE Trans. Intell. Transp. Syst., **2022**, *23*: 10945−10956. doi: 10.1109/TITS.2021.3097356
9. Ploeg, J.; Van De Wouw, N.; Nijmeijer, H. L_p string stability of cascaded systems: Application to vehicle platooning. *IEEE Trans. Control Syst. Technol*. **2014**, *22*, 786–793. doi:10.1109/TCST.2013.2258346
10. Ploeg, J.; Shukla, D.P.; Van De Wouw, N.; *et al*. Controller synthesis for string stability of vehicle platoons. IEEE Trans. Intell. Transp. Syst., **2014**, *15*: 854−865. doi: 10.1109/TITS.2013.2291493
11. Guo, G.; Li, D.D. Adaptive sliding mode control of vehicular platoons with prescribed tracking performance. IEEE Trans. Veh. Technol., **2019**, *68*: 7511−7520. doi: 10.1109/TVT.2019.2921816
12. Zhang, X.H.; Sun, J.; Zheng, Z.D.; *et al*. On the string stability of neural network-based car-following models: A generic analysis framework. Transp. Res. Part C Emerging Technol., **2024**, *160*: 104525. doi: 10.1016/j.trc.2024.104525
13. Zheng, Y.; Xu, M.; Wu, S.N.; *et al*. Development of connected and automated vehicle platoons with combined spacing policy. IEEE Trans. Intell. Transp. Syst., **2023**, *24*: 596−614. doi: 10.1109/TITS.2022.3216618
14. Li, S.E.; Zheng, Y.; Li, K.Q.; *et al*. Dynamical modeling and distributed control of connected and automated vehicles: Challenges and opportunities. IEEE Intell. Transp. Syst. Mag., **2017**, *9*: 46−58. doi: 10.1109/MITS.2017.2709781
15. Mousavinejad, E.; Yang, F.W.; Han, Q.L.; *et al*. Distributed cyber attacks detection and recovery mechanism for vehicle platooning. IEEE Trans. Intell. Transp. Syst., **2020**, *21*: 3821−3834. doi: 10.1109/TITS.2019.2934481
16. Ge, X.H.; Xiao, S.Y.; Han, Q.L.; *et al*. Dynamic event-triggered scheduling and platooning control co-design for automated vehicles over vehicular ad-hoc networks. IEEE/CAA J. Autom. Sin., **2022**, *9*: 31−46. doi: 10.1109/JAS.2021.1004060
17. Lei, L.; Liu, T.; Zheng, K.; *et al*. Deep reinforcement learning aided platoon control relying on V2X information. IEEE Trans. Veh. Technol., **2022**, *71*: 5811−5826. doi: 10.1109/TVT.2022.3161585
18. Zhu, Z.R.; Chai, Y.; Yang, Z.M.; *et al*. Exponential-alpha safety criteria of a class of dynamic systems with barrier functions. IEEE/CAA J. Autom. Sin., **2022**, *9*: 1939−1951. doi: 10.1109/JAS.2020.1003408
19. Jain, V.; Liu, D.; Baldi, S. Adaptive strategies to platoon merging with vehicle engine uncertainty. IFAC Pap. OnLine, **2020**, *53*: 15065−15070. doi: 10.1016/j.ifacol.2020.12.2027
20. Ge, X.H.; Han, Q.L.; Zhang, M.X.; *et al*. Communication resource-efficient vehicle platooning control with various spacing policies. IEEE/CAA J. Autom. Sin., **2024**, *11*: 362−376. doi: 10.1109/JAS.2023.123507
21. Liu, Y.; Xu, L.W.; Cai, G.S.; *et al*. Distributed robust platooning control for heterogeneous vehicle group under parametric uncertainty and hybrid attacks. IEEE Trans. Veh. Technol., **2023**, *72*: 5677−5689. doi: 10.1109/TVT.2022.3231618
22. Feng, G.; Dang, D.F.; He, Y.D. Robust coordinated control of nonlinear heterogeneous platoon interacted by uncertain topology. IEEE Trans. Intell. Transp. Syst., **2022**, *23*: 4982−4992. doi: 10.1109/TITS.2020.3045107
23. Xiao, S.Y.; Ge, X.H.; Han, Q.L.; *et al*. Secure distributed adaptive platooning control of automated vehicles over vehicular Ad-Hoc networks under denial-of-service attacks. IEEE Trans. Cybern., **2022**, *52*: 12003−12015. doi: 10.1109/TCYB.2021.3074318
24. Biroon, R.A.; Biron, Z.A.; Pisu, P. False data injection attack in a platoon of CACC: Real-time detection and isolation with a PDE approach. IEEE Trans. Intell. Transp. Syst., **2022**, *23*: 8692−8703. doi: 10.1109/TITS.2021.3085196
25. Su, Y.F.; Cai, H.; Huang, J. The cooperative output regulation by the distributed observer approach. Int. J. Network Dyn. Intell., **2022**, *1*: 20−35. doi: 10.53941/ijndi0101003
26. Baldi, S.; Liu, D.; Jain, V.; *et al*. Establishing platoons of bidirectional cooperative vehicles with engine limits and uncertain dynamics. IEEE Trans. Intell. Transp. Syst., **2021**, *22*: 2679−2691. doi: 10.1109/TITS.2020.2973799
27. Feng, S.; Zhang, Y.; Li, S.B.; *et al*. String stability for vehicular platoon control: Definitions and analysis methods. Annu. Rev. Control, **2019**, *47*: 81−97. doi: 10.1016/j.arcontrol.2019.03.001
28. Pan, D.F.; Ding, D.R.; Ge, X.H.; *et al*. Privacy-preserving platooning control of vehicular cyber-physical systems with saturated inputs. IEEE Trans. Syst. Man Cybern. Syst., **2023**, *53*: 2083−2097. doi: 10.1109/TSMC.2022.3226901
29. Liu, A.Q.; Li, T.; Gu, Y.; Dai, H. Cooperative extended state observer based control of vehicle platoons with arbitrarily small time headway. Automatica, **2021**, *129*: 109678. doi: 10.1016/j.automatica.2021.109678

Citation: Pan, D. String Stable Bidirectional Platooning Control for Heterogeneous Connected Automated Vehicles. *International Journal of Network Dynamics and Intelligence*. 2024, 3(4), 100026. doi: 10.53941/ijndi.2024.100026